Published OnlineFirst April 24, 2018; DOI: 10.1158/1940-6207.CAPR-17-0268

Research Article

Cancer Prevention Research

Evaluation of Biodistribution of Sulforaphane after Administration of Oral Broccoli Sprout Extract in Melanoma Patients with Multiple Atypical Nevi

Shawn Tahata[1], Shivendra V. Singh[1,2], Yan Lin[1], Eun-Ryeong Hahm[2], Jan H. Beumer[1,3,4], Susan M. Christner[1], Uma N. Rao[1], Cindy Sander[1], Ahmad A. Tarhini[5], Hussein Tawbi[6], Laura K. Ferris[7], Melissa Wilson[1], Amy Rose[1], Catherine M. Dietz[8], Ellen Hughes[8], Jed W. Fahey[9], Sancy A. Leachman[10], Pamela B. Cassidy[10], Lisa H. Butterfield[1,3], Hassane M. Zarour[1,3], and John M. Kirkwood[1,3]

Abstract

Broccoli sprout extract containing sulforaphane (BSE-SFN) has been shown to inhibit ultraviolet radiation–induced damage and tumor progression in skin. This study evaluated the toxicity and potential effects of oral BSE-SFN at three dosages. Seventeen patients who each had at least 2 atypical nevi and a prior history of melanoma were randomly allocated to 50, 100, or 200 μmol oral BSE-SFN daily for 28 days. Atypical nevi were photographed on days 1 and 28, and plasma and nevus samples were taken on days 1, 2, and 28. Endpoints assessed were safety, plasma and skin sulforaphane levels, gross and histologic changes, IHC for phospho-STAT3(Y705), Ki-67, Bcl-2, HMOX1, and TUNEL, plasma cytokine levels, and tissue proteomics. All 17 patients completed 28 days with no dose-limiting toxicities. Plasma sulforaphane levels pooled for days 1, 2, and 28 showed median postadministration increases of 120 ng/mL for 50 μmol, 206 ng/mL for 100 μmol, and 655 ng/mL for 200 μmol. Median skin sulforaphane levels on day 28 were 0.0, 3.1, and 34.1 ng/g for 50, 100, and 200 μmol, respectively. Plasma levels of proinflammatory cytokines decreased from day 1 to 28. The tumor suppressor decorin was increased from day 1 to 28. Oral BSE-SFN is well tolerated at daily doses up to 200 μmol and achieves dose-dependent levels in plasma and skin. A larger efficacy evaluation of 200 μmol daily for longer intervals is now reasonable to better characterize clinical and biological effects of BSE-SFN as chemoprevention for melanoma. *Cancer Prev Res; 11(7); 429–38. ©2018 AACR.*

Introduction

Despite public health efforts to promote ultraviolet radiation avoidance and sun-protective behaviors, the annual incidence of melanoma continues to rise faster than that of any other of the seven most common cancers. Melanoma is currently the sixth most frequently diagnosed cancer in the United States (1), and although it comprises only 4% of skin cancer cases, it is responsible for 80% of skin cancer–related deaths (2). An important risk factor for melanoma is the presence of atypical (formerly known as dysplastic) nevi, which are pigmented lesions that, although benign, share several clinical features with melanoma, such as larger size (usually $\geq$6 mm), border irregularity, and color variegation (3, 4). Atypical nevi can be sporadic or associated with familial syndromes, such as the familial atypical multiple-mole melanoma (FAMMM) syndrome (4, 5).

Although most atypical nevi do not progress to melanoma, having multiple atypical nevi is associated with a

[1]UPMC Hillman Cancer Center, University of Pittsburgh, Pittsburgh, Pennsylvania. [2]Department of Pharmacology and Chemical Biology, University of Pittsburgh School of Medicine, Pittsburgh, Pennsylvania. [3]Department of Medicine, University of Pittsburgh School of Medicine, Pittsburgh, Pennsylvania. [4]Department of Pharmaceutical Sciences, University of Pittsburgh School of Pharmacy, Pittsburgh, Pennsylvania. [5]Cleveland Clinic Taussig Cancer Institute, Cleveland, Ohio. [6]Department of Melanoma Medical Oncology, University of Texas MD Anderson Cancer Center, Houston, Texas. [7]Department of Dermatology, University of Pittsburgh, Pittsburgh, Pennsylvania. [8]Computer Vision Group, Veytel, LLC, Pittsburgh, Pennsylvania. [9]Department of Medicine, Johns Hopkins University School of Medicine, Baltimore, Maryland. [10]Knight Cancer Institute, Oregon Health and Science University, Portland, Oregon.

Note: Supplementary data for this article are available at Cancer Prevention Research Online (http://cancerprevres.aacrjournals.org/).

Corresponding Author: John M. Kirkwood, University of Pittsburgh School of Medicine, University of Pittsburgh Cancer Institute, 5117 Centre Avenue, Suite 1.32, Pittsburgh, PA 15213. Phone: 412-623-7707; Fax: 412-623-7704; E-mail: kirkwoodjm@upmc.edu

doi: 10.1158/1940-6207.CAPR-17-0268

Published OnlineFirst April 24, 2018; DOI: 10.1158/1940-6207.CAPR-17-0268

significantly increased risk of melanoma, with FAMMM syndrome conferring a lifetime risk between 28% and 69% (6, 7). In addition, patients with atypical nevi and a prior history of melanoma have an approximately 8-fold increased risk of developing new melanoma (8). For high-risk patients such as these, ultraviolet radiation–protective measures alone are insufficient as a preventive strategy, and risk-modifying therapies such as chemoprevention are reasonable to develop. Chemoprevention as applied to melanoma may use natural or synthetic agents to delay, reverse, or suppress premalignant lesions from progressing to invasive cancer and can include primary prevention for high-risk individuals without a history of melanoma or secondary or tertiary prevention in those with premalignant lesions or cured malignancies, respectively (9). Although many candidate agents, including lipid-lowering statins and fibrates, retinoids, NSAIDs, cytokines and IFNs, and vitamin E have shown promise in laboratory and early population studies, most have not been studied in randomized controlled trials, and their use as chemopreventive agents is not currently supported by the available data (10, 11).

Epidemiologic studies have demonstrated an inverse correlation between consumption of cruciferous vegetables and the risk of cancer at multiple organ sites (12–15). This protective effect is attributed to organic isothiocyanates derived from glucosinolates found in cruciferous vegetables. Sulforaphane is an isothiocyanate that has been well studied for its anticancer properties, which have been attributed to its effects on multiple cellular targets involved in the initiation (inhibition of drug metabolizing phase I enzymes and induction of phase II enzymes), promotion (induction of apoptosis and cell-cycle inhibition), and progression (inhibition of angiogenesis and metastasis) of cancer development (16–18). One such target, STAT3, is known to be activated in the progression of melanoma and other solid tumors (19–22), and its modulation by IFNα-2b has been shown to play a central role in the neoadjuvant antitumor effect of this therapy in metastatic melanoma (23–25). Constitutive activation of STAT3 has also been demonstrated in atypical nevi and correlates with the degree of pathologic atypia observed (25).

Topical application of broccoli sprout extract containing sulforaphane (BSE-SFN) has been shown to modulate STAT3 activity in cancer cells, inhibit chemically induced skin tumors and reduce ultraviolet radiation–induced skin erythema in mice and humans (25–28). BSE-SFN has also been shown to induce the transcription factor Nrf2, which enhances the expression of cytoprotective enzymes such as heme oxygenase 1 (HMOX1), GST, and NAD(P)H:quinone oxidoreductase 1 (28). Oral preparations of BSE-SFN have the added advantage of systemic modulation of precursor lesions, greater ease of administration, improved patient adherence, and reduced overall costs. For patients with large numbers of atypical nevi for whom topical application would be impractical, oral preparations are a more feasible alternative. This study used an oral formulation of BSE-SFN developed by Talalay and colleagues extracted from *Brassica oleracea* and analyzed for the concentration of isothiocyanates and glucosinolates using previously described methods (29–31). This formulation, administered as a gel capsule, contains 20 to 50 times the glucosinolate precursors found in mature plants and has been shown to be well tolerated by humans with no adverse effects or drug interactions with doses up to 200 μmol (31, 32). In this study, we evaluate the feasibility of oral BSE-SFN administration for patients at elevated risk for melanoma at three dosages spanning the range reported in the literature (31, 33–35), document the resulting sulforaphane levels in plasma and, for the first time, in skin, and report preliminary observations of its biological impact upon atypical nevi.

Materials and Methods

Patient selection

Eligible patients had at least two clinically atypical nevi $\geq$4 mm in diameter and a previous diagnosis of cutaneous melanoma. None had received any form of systemic antineoplastic treatment for melanoma within a year prior to day 1 of treatment in this study. Subjects were at least 12 years of age and did not have any known allergies to cruciferous vegetables; all agreed to abstain from dietary sources of glucosinolates and isothiocyanates beginning 3 days prior to the study and throughout the duration of the active study (28 days). Participants were asked to keep a food diary and to record instances of accidental ingestion of these foods and were removed from the study if this occurred more than 7 times. Patients with clinically significant abnormalities on initial complete blood count or complete metabolic panel or positive serum pregnancy test were excluded.

Study design

The study population was randomly divided into three dosage groups receiving 50, 100, and 200 μmol of oral BSE-SFN once daily for 28 days. Randomization was stratified by the number of atypical nevi on each patient to ensure each arm contained a roughly equal number of patients with various numbers of atypical nevi. Patients were instructed to take each dose at 10 am $\pm$ 2 hours prior to consumption of other foods and fluids, and to fast after midnight on days preceding skin biopsy. Prior to starting treatment, 2 to 6 atypical nevi $\geq$4 mm in diameter were photographed for each subject and ranked visually in descending order of clinical features of atypia. Any nevi or lesions suspicious for incipient melanoma were removed and not intended for study. Excisional or large punch biopsy of an atypical nevus and surrounding normal skin was performed on days 1 and 28 at 2 hours $\pm$ 30 minutes

Published OnlineFirst April 24, 2018; DOI: 10.1158/1940-6207.CAPR-17-0268

after administration of BSE-SFN. An additional biopsy was done on day 2 for patients with ≥3 atypical nevi. Photographic documentation was obtained prior to each biopsy. Blood samples were drawn on days 1, 2 (if biopsy was done), and 28 before and 2 hours ± 30 minutes after administration of BSE-SFN. Informed consent was obtained from all study participants prior to enrollment. This study was approved by the University of Pittsburgh Institutional Review Board (protocol 10-114) and performed under Investigational New Drug (IND) number 112691.

Laboratory methods

Sample preparation. After biopsy, skin samples were immediately immersed in saline and held on ice. Specimens were evaluated and then dissected by a designated pathologist or dermatopathologist of the Melanoma Program of the UPMC Hillman Cancer Center (Pittsburgh, PA). Part of the atypical nevus was used to confirm the diagnosis, and the remainder was immediately snap-frozen in liquid nitrogen at −140°C, with the remaining nevus tissue used in IHC and other molecular analyses and the surrounding normal skin used to assess tissue sulforaphane levels. Blood samples taken pre- and post–BSE-SFN administration were collected in 6 mL K_2EDTA lavender top tubes (BD Hemogard, 367863). Samples were centrifuged at 2,000 × *g* for 10 minutes at 4°C, and plasma was subsequently stored at −80°C until analyzed.

Determination of sulforaphane levels in plasma and skin. Sulforaphane levels in plasma were measured using a liquid chromatographic-tandem mass spectrometric assay based on previously published methods (36). To 100 μL of plasma sample, [D_8]-sulforaphane (Toronto Research Chemicals, S699117) was added, followed by 500 μL of methanol for protein precipitation. This method had a dynamic range of 10 to 3,000 ng/mL for plasma. There was a significant difference between freshly prepared quality control samples relative to same quality controls processed after being frozen at −80°C. Up to three freeze-thaw cycles were tested and shown to result in appropriate assay performance. To correct for this and allow analysis of the clinical samples that were kept frozen until analyzed, all standard calibrators were prepared the day prior to analysis and stored at −80°C to be run along with frozen quality control samples. On the basis of quality control samples at 10, 25, 250, and 2,500 ng/mL, the precision ranged from 2.0% to 7.2% and the accuracy ranged from −12.0% to 11.6%. The normal skin portion of each skin biopsy was homogenized with 4 parts (v/g) of PBS and analyzed as described for plasma. Tissue sulforaphane concentrations were adjusted to account for this dilution during sample preparation.

IHC and other molecular methods. Snap-frozen nevus tissues were embedded in optimal cutting temperature compound then sectioned at 4 to 5 μm and fixed in acetone. IHC staining of phospho-STAT3 (Y705; hereafter referred to as pSTAT3), Ki-67 (proliferation marker), and Bcl-2 (antiapoptotic marker) was performed as described previously (36, 37). For biopsies with sufficient tissue, staining for HMOX1 (downstream target of Nrf2) was also performed. The sections were then counterstained with hematoxylin and examined. Evidence of apoptosis in nevus specimens was evaluated using the ApopTag Plus Peroxidase *In Situ* Apoptosis Kit (Millipore, S7101), a terminal deoxynucleotidyl transferase dUTP nick end labeling (TUNEL) assay. For each IHC stain, positive controls were performed, but negative controls were not performed as no unexpected findings were revealed, in accordance with institutional protocols. Staining for pSTAT3, Ki-67, Bcl-2, HMOX1, and TUNEL in nevic melanocytes, keratinocytes, lymphocytes, and endothelial cells was determined independently by a pathologist, with day 1, 2, and 28 samples compared in a blinded fashion. Staining for pSTAT3, Bcl-2, and TUNEL was graded as very strong (4+), strong or positive (3+), moderate or weakly positive (2+), less or few positive (1+), or negative (0); Ki-67 and HMOX1 were graded as positive (1+) or weakly positive or negative (0).

Cytokine concentrations were measured in plasma on day 1 pretreatment and on day 28 posttreatment in duplicate using the Cytokine Human 30-Plex Panel for Luminex Platform (Invitrogen, LHC6003). Concentrations were determined with the kit standard curves per the manufacturer's instructions, and concentrations below the lower limit of quantification (LLQ) were taken to equal zero. The UPMC Hillman Cancer Center Immunologic Monitoring and Cellular Products Laboratory participates in Luminex external proficiency panels to ensure optimal data quality. Pairs of nevus tissue from 6 patients on days 1 and 28 were used for proteomic analysis by two-dimensional gel electrophoresis followed by matrix-assisted laser desorption/ionization—time-of-flight mass spectrometry as described by us previously (38). Details of tissue processing, CyDye labeling, two-dimensional gel electrophoresis, image scan and data analysis, spot picking and trypsin digestion, and mass spectrometry were the same as described previously (38).

Assessment of gross morphologic response. Paired photographs of atypical nevi for each subject at baseline and on day 28 were evaluated using digital image analysis for changes in ABCD features including size parameters (i.e., area, perimeter, diameter), shape asymmetry, border irregularity, and color asymmetry. A millimeter-scaled ruler was included in each photograph for scale. The borders of the nevi were defined using supervised segmentation and used to compute size parameters. Color asymmetry was assessed by comparing the change of the mean color saturation across the four quadrants of the nevi, defined by the major

Published OnlineFirst April 24, 2018; DOI: 10.1158/1940-6207.CAPR-17-0268

Table 1. Relevant patient characteristics by dosage group

	BSE-SFN dosage group		
	50 μmol ($n = 6$)	**100 μmol ($n = 6$)**	**200 μmol ($n = 5$)**
Sex (female)	3 *(50%)*	4 *(67%)*	5 *(100%)*
Age (median)	46 yrs.	51 yrs.	44 yrs.
Race (Caucasian)	6 *(100%)*	6 *(100%)*	5 *(100%)*
Prior melanoma history, by stage	MIS (1) Stage I (4) Stage II (2)	MIS (1) Stage I (3) Stage III (1) unstageable (1)	Stage I (4) Stage III (1)

Abbreviation: MIS, melanoma *in situ*.

and minor axes. Shape asymmetry was assessed by calculating the ratio of pixels outside the symmetric components of the nevi to those pixels within the symmetric components of the nevi (i.e., portions that completely overlap when the nevus is folded across the major and minor axes). Border irregularity was computed as the ratio of the area of the nevus shape to the area of a convex hull that best fits the nevus shape. A demonstration of these techniques is included in Fig. 3.

Assessment of histologic response. A portion of each biopsy of an atypical nevus and adjacent normal skin was stained with hematoxylin and eosin and submitted for histologic examination. Biopsy samples from days 1 and 28 were evaluated by a dermatopathologist for features of cytologic atypia (graded as absent, mild, moderate, or severe) and for tumor-infiltrating lymphocytes (graded as absent, moderate, or brisk).

Statistical analysis and adverse event reporting

Endpoints of interest for this study were sulforaphane concentrations in plasma and skin; gross and histologic changes in atypical nevi; pSTAT3, Ki-67, Bcl-2, and HMOX1 expression and TUNEL as determined by IHC; plasma cytokine levels; and protein expression as determined by proteomic analysis. Any measurements found to be below the LLQ were taken to equal zero. For numerical data, descriptive statistics were used to summarize the distribution of each endpoint of interest at each time point and, if appropriate, at each dose level. The pre- and posttreatment difference in the values for a specific measurement of two nevi from the same patient was used to measure the treatment effect. Statistical significance was determined using the Student *t* test for proteomic analysis and Wilcoxon signed rank test for all other analyses. All adverse events were tabulated using the NCI common terminology criteria for adverse events.

Results

Patient characteristics

The study enrolled 17 patients from September 2012 to August 2015. Relevant patient characteristics are listed in Table 1. All of the patients completed 28 days at 50, 100, or 200 μmol dosages of BSE-SFN. Twelve patients were female and 5 were male; the median age was 47 (range, 22–66). All patients were of Caucasian descent. Five patients had 2 atypical nevi and 12 had $\geq$3 atypical nevi on initial evaluation. Prior melanoma history included melanoma *in situ* in 2 patients, stage I disease in 11 patients, stage II in 1 patient, stage III in 2 patients, and unstageable disease in 1 patient. No patients were removed from the study for excessive consumption of glucosinolate or isothiocyanate-containing foods.

Sulforaphane levels in plasma and skin

Median plasma sulforaphane levels on days 1, 2, and 28 for the 50, 100, and 200 μmol groups pre- and post–BSE-SFN administration are depicted in Fig. 1A. At baseline prior to BSE-SFN administration, plasma sulforaphane levels were undetectable in all but one patient. After pooling data from days 1, 2, and 28 for each dosage group, the median posttreatment increase in plasma sulforaphane concentration was 120 (range, −182–208), 206 (range, 89–420), and 656 (range, 396–1,305) ng/mL for the 50, 100, and 200 μmol groups, respectively (Supplementary Table S1).

Median skin sulforaphane levels on days 1, 2, and 28 for the 50, 100, and 200 μmol groups post–BSE-SFN administration are depicted in Fig. 1B. All but one skin sample yielded initial sulforaphane levels that were below our assay's LLQ (10 ng/g). Of these, one sample from day 1, seven from day 2, and nine from day 28 produced distinct peaks on mass spectrometry that fell within the assay's dynamic range after adjusting for sample dilution. Median posttreatment tissue sulforaphane levels on day 28 were 0.0 ng/g (range, 0.0–21.8) for 50 μmol, 3.1 ng/g (range, 0.0–18.9) for 100 μmol, and 34.1 ng/g (range, 0.0–63.6) for 200 μmol (Supplementary Table S2). Three samples at day 28, one from each dose group, produced sulforaphane peaks that still fell below our LLQ even after adjusting for sample dilution. For the purposes of data tabulation, levels below LLQ were taken to equal zero. Both plasma and skin sulforaphane levels demonstrated a dose–response relationship.

IHC and molecular response

No consistent alterations in IHC staining were observed from day 1 to 28, with results analyzed both for the study group as a whole and stratified by dosage (Fig. 2). pSTAT3 was strongly expressed in endothelial cells at baseline and on day 28 in all dosage groups; however, nevic expression of pSTAT3 was not observed in the majority of samples.

Published OnlineFirst April 24, 2018; DOI: 10.1158/1940-6207.CAPR-17-0268

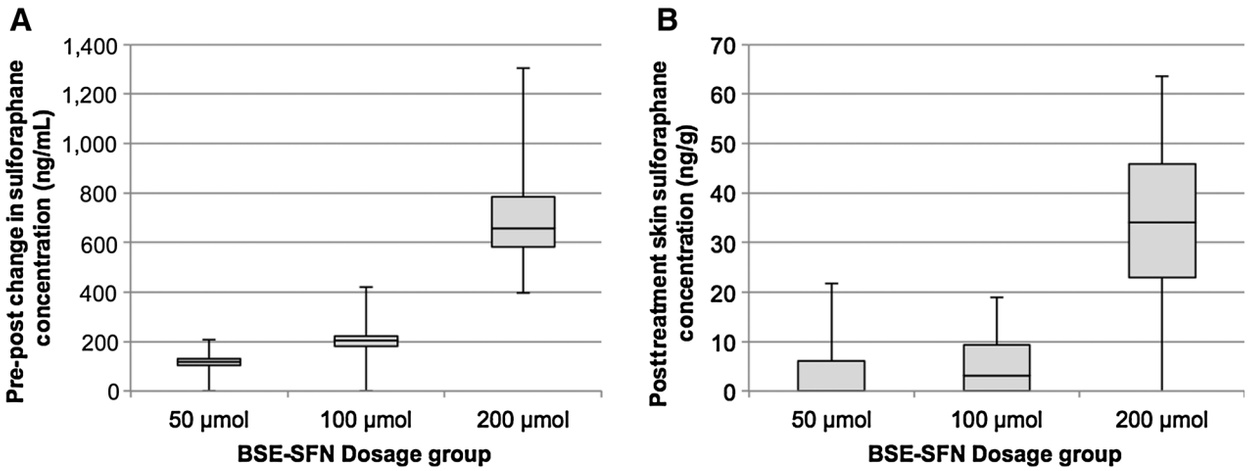

Figure 1.

A, Posttreatment increase in plasma sulforaphane concentration, stratified by dose group. **B,** Day 28 posttreatment skin sulforaphane concentration, stratified by dose group. Data are presented in box plots.

Ki-67 was expressed at baseline and on day 28 in keratinocytes but only rarely in nevic melanocytes. Bcl-2 was expressed most prominently in nevi but occasionally in other cell types, including lymphocytes. HMOX1 was negative in nevic melanocytes in all 11 of the paired samples in which it was examined. TUNEL assay was occasionally positive in nevus, normal epidermis, and endothelial cells.

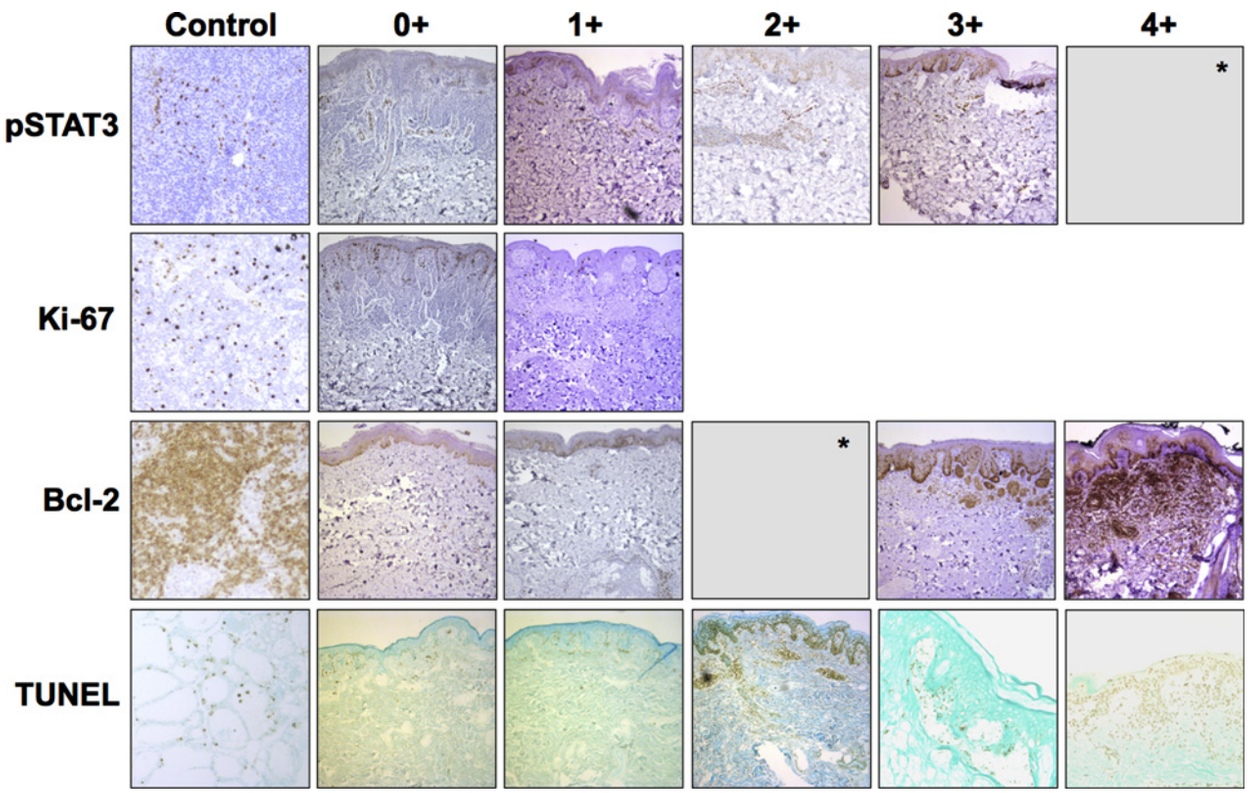

Figure 2.

Representative skin biopsy specimens with IHC staining for pSTAT3, Ki-67, Bcl-2, and TUNEL showing varying degrees of positivity in nevic melanocytes, with positive controls. pSTAT3, Bcl-2, and TUNEL were graded as 0+ (negative), 1+ (less or few positive), 2+ (moderate or weakly positive), 3+ (strong or positive), or 4+ (very strong); Ki-67 was graded as 0+ (negative) or 1+ positive. IHC for heme oxygenase not shown. *, No specimens demonstrated 4+ pSTAT3 staining or 2+ Bcl-2 staining. Images were obtained at 10× objective magnification using a Leica microscope.

Published OnlineFirst April 24, 2018; DOI: 10.1158/1940-6207.CAPR-17-0268

Table 2. Plasma cytokine levels on days 1 (pre–BSE-SFN administration) and 28 (post–BSE-SFN administration) with percent change (data pooled from all dosage groups)

	Median cytokine concentration (pg/mL)		Percent change in cytokine concentration*
	Day 1	Day 28	
EGF	26	19.5	−25.0
Exotaxin	22.5	18.5	−17.8
bFGF	29	23	−20.6
G-CSF	504.3	462	−8.4
GM-CSF	0	0	0.0
HGF	352	324	−8.0
IFNα	81	65	−19.8
IFNγ	46.5	37.5	−19.4
IL18	34	28.5	−16.2
IL-1RA	162	139.5	−13.9
IL2	11.5	11	−4.3
IL2R	471.5	341.5	−47.6
IL4	0	0	0.0
IL5	13	7	−46.2
IL6	6	0	−100.0
IL7	0	0	0.0
IL8	14	0	−100.0
IL10	0	0	0.0
IL12	223	218	−2.2
IL13	22.5	20	−11.1
IL15	0	86	—
IL17	0	0	0.0
IP-10	22	21	−4.5*
MCP-1	231.5	211.5	−8.6*
MIG	113	84.5	−25.2*
MIP-1α	79.5	65	−18.2
MIP-1β	75	62	−17.3*
RANTES	3,766	3,266	−13.3
TNFα	10	6.5	−35.0
VEGF	0	0	0.0

NOTE: Cytokine levels were measured using the Cytokine Human 30-Plex Panel for Luminex Platform.

*, Values that are statistically significant by the Wilcoxon signed rank test.

Statistically significant decreases in the proinflammatory cytokines IP-10 (CXCL10), MCP-1 (CCL-2), MIG (CXCL9), and MIP-1β (CCL-4) were observed between days 1 and 28 (Table 2). All four of these cytokines serve as chemoattractants for immune cells, including monocytes, T cells, and natural killer cells. In addition, IFNγ, which induces the secretion of IP-10 and MIG, was decreased in day 28 samples, and this decrease approached statistical significance. The cytokine results were not correlated with BSE-SFN dosage due to limited sample size. Of 92 proteins identified with proteomic analysis, 14 distinct proteins, including, notably, the tumor suppressor decorin, were found to have significant changes in average expression in day 28 nevi as compared with day 1 nevi, defined as an average ratio ≥ 1.5 and $P \leq 0.10$ (Table 3).

Gross morphologic response

The digital image analysis for ABCD features demonstrated measurable changes from baseline to day 28. On average, the nevi increased slightly in size (i.e., diameter, perimeter, and area), although some individual nevi decreased in size. This overall increase in size was generally less pronounced in the higher BSE-SFN dosage groups and an apparent trend toward reduced enlargement in size with increased BSE-SFN dose was observed, with the most notable effect observed in the 200 μmol dose group. This trend, however, did not achieve statistical significance. No obvious trends in changes in color asymmetry, shape asymmetry, and border irregularity were observed. Representative examples of nevi with observed gross changes are depicted in Fig. 3.

Histologic response

In 6 nevus pairs, an increase in cytologic atypia was observed from days 1 to 28. A decrease in cytologic atypia was observed in 2 pairs. Tumor-infiltrating lymphocytes decreased in 2 pairs and increased in 2 pairs. Five pairs were unable to be evaluated because of inadequate tissue staining. Overall, no consistent changes in cytologic atypia and tumor-infiltrating lymphocytes were noted between day 1 and 28 specimens.

Safety assessment

No dose-limiting toxicities of BSE-SFN were observed. Grade 2 nausea occurred in one patient in the 200 μmol dosage group. No other adverse events were reported.

Discussion

In this study, we show that oral BSE-SFN is well tolerated at three doses ranging from 50 to 200 μmol daily and achieves dose-dependent concentrations in plasma and skin. Tissue levels of sulforaphane achieved with the 200 μmol dose are equivalent to those on the lower end of the dose–response curve in previous studies (27, 39) but nevertheless were significantly lower than our corresponding plasma levels. Previous research has shown that sulforaphane tissue concentrations after oral administration differ depending on the end organ (40). The lower concentrations of sulforaphane in skin relative to those in plasma may reflect the relatively poor perfusion of skin compared with other organs (41, 42) and may require increased dosage or more frequent dosing to achieve higher sustained tissue levels.

IHC analysis was limited in this pilot study due to small sample size and short treatment duration. In addition, because many of the nevus biopsies were of small size and tissue sampling for diagnosis and measuring sulforaphane levels took precedence, the remaining tissue was occasionally less than optimal for subsequent IHC analyses. However, alterations in plasma levels of select inflammatory cytokines and in tissue levels of the tumor suppressor decorin provide preliminary evidence for the biochemical activity of oral sulforaphane in the cutaneous nevi of patients with a history of melanoma.

Although the gross changes in nevi observed in this study are encouraging, it is worth noting that appreciable changes in the gross appearance of nevi in one month are unusual, and other factors such as interval sun exposure and variation in angle or lighting during photography may

Published OnlineFirst April 24, 2018; DOI: 10.1158/1940-6207.CAPR-17-0268

Table 3. Changes in nevus protein expression after oral administration of BSE-SFN in comparison with pretreatment

		Day 28/day 0	
Assigned ID	**Protein name**	***P***	**Av. ratio**
22	Keratin, type II cytoskeletal 1 OS = *Homo sapiens* GN = KRT1 PE = 1 SV = 6	0.058	1.7
33	Fibrinogen gamma chain OS = *Homo sapiens* GN = FGG PE = 1 SV = 3	0.0071	1.5
34	Fibrinogen gamma chain OS = *Homo sapiens* GN = FGG PE = 1 SV = 3	0.013	1.7
35	Fibrinogen gamma chain OS = *Homo sapiens* GN = FGG PE = 1 SV = 3	0.0037	1.7
37	Vimentin OS = *Homo sapiens* GN = VIM PE = 1 SV = 4	0.034	1.8
41	Septin-2 OS = *Homo sapiens* GN = SEPT2 PE = 1 SV = 1	0.069	1.5
45	Alpha-enolase OS = *Homo sapiens* GN = ENO1 PE = 1 SV = 2	0.047	1.5
46	Decorin OS = *Homo sapiens* GN = DCN PE = 1 SV = 1	0.0051	1.6
53	Fibrinogen beta chain OS = *Homo sapiens* GN = FGB PE = 1 SV = 2	0.015	1.6
58	Decorin OS = *Homo sapiens* GN = DCN PE = 1 SV = 1	0.067	1.5
59	Delta-aminolevulinic acid dehydratase OS = *Homo sapiens* GN = ALAD PE = 1 SV = 1	0.0077	1.5
68	Carbonic anhydrase 1 OS = *Homo sapiens* GN = CA1 PE = 1 SV = 2	0.067	−1.7
69	Rho GDP-dissociation inhibitor 1 OS = *Homo sapiens* GN = ARHGDIA PE = 1 SV = 3	0.082	1.6
76	Phosphatidylethanolamine-binding protein 1 OS = *Homo sapiens* GN = PEBP1 PE = 1 SV = 3	0.091	1.7
78	Peroxiredoxin-2 OS = *Homo sapiens* GN = PRDX2 PE = 1 SV = 5	0.078	1.5
85	Galectin-7 OS = *Homo sapiens* GN = LGALS7 PE = 1 SV = 2	0.075	−1.8
87	Apolipoprotein C-III OS = *Homo sapiens* GN = APOC3 PE = 1 SV = 1	0.075	−1.6

NOTE: Six pairs of nevus tissues from days 0 and 28 (3 from 50 μmol group, 2 from 100 μmol group, and 1 from 200 μmol group) were used for proteomics by two-dimensional gel electrophoresis followed by MALDI-TOF/TOF. Altered proteins in day 28 specimens compared with day 0 specimens are listed. The cut-off criteria for selection were ≥1.5-fold difference and *P* value less than 0.10 by two-sided Student *t* test. Multiple spots for fibrinogen gamma chain and decorin suggest posttranslational modification.

Abbreviations: GN, gene name; OS, organism name; PE, protein existence; SV, sequence version.

have contributed to these perceived changes. The use of a dermatoscope may help to standardize lesion visualization and will be considered for future studies. Another limitation of this study was that different nevi were assessed on days 1 and 28 to evaluate the histologic response. Serial biopsy of a single nevus was not performed because of concerns that repeated biopsy and the associated traumatic changes would alter the immunologic milieu of the tissue. Consequently, our assessment of the treatment effect on histologic features such as cytologic atypia and tumor-infiltrating lymphocytes may have been limited by interlesional heterogeneity. Histopathologic analysis of

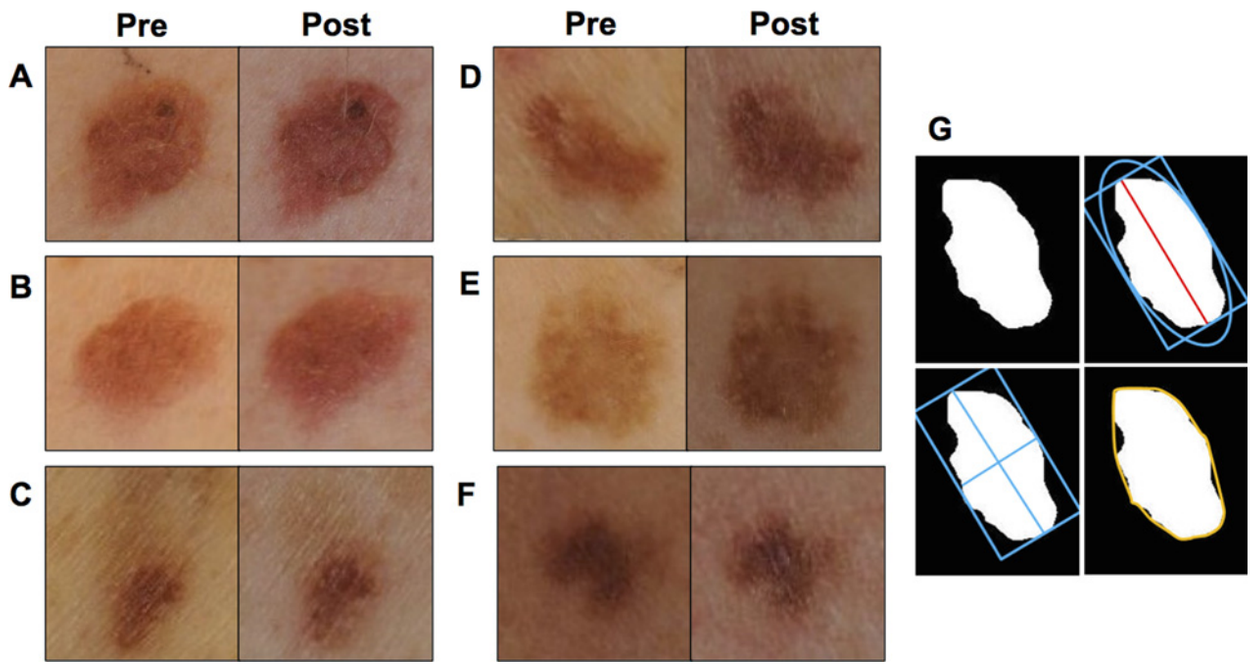

Figure 3.

Paired representative gross photographic images of nevi pre- and posttreatment demonstrating various gross changes, including increase in size but decrease in color asymmetry (**A**), increase in shape asymmetry (**B**), increase in border irregularity (**C**), increase in color asymmetry (**D**), decrease in size (**E**), and decrease in shape asymmetry and border irregularity (**F**). **G,** Demonstration of image analysis techniques used to delineate border (top left), diameter (top right), major and minor axes (bottom left), and convex hull (bottom right).

Published OnlineFirst April 24, 2018; DOI: 10.1158/1940-6207.CAPR-17-0268

samples obtained through skin biopsy remains the gold standard for the diagnosis of melanoma and other pigmented skin lesions. However, the prospect for gene expression studies to assist in diagnosis is raised by a recently reported two-gene molecular assay using noninvasive adhesive patch biopsy (43), which circumvents some of the limitations of serial biopsy and may merit consideration for future studies of BSE-SFN and other candidate chemopreventive agents.

The results of this pilot study support the potential biological impact of BSE-SFN and its putative biological mechanisms that are relevant for chemoprevention in atypical nevi, and by extension, melanoma. Notably, this is the first study of its kind to document the concentration of sulforaphane in skin after oral administration of BSE-SFN and opens up an array of possible applications for oral BSE-SFN as a chemoprotective agent not only for melanoma but also for a variety of other skin-related conditions. Because oral BSE-SFN has been shown to have an excellent safety profile and to achieve dose-dependent concentrations in plasma and skin, these results argue for a larger phase II study of oral BSE-SFN at 200 μmol daily over a longer treatment period, such as 3 to 6 months or longer. Considering the relatively low tissue concentrations achieved at our maximum dosage of 200 μmol, higher doses or more frequent dosing of BSE-SFN are also reasonable to consider. In this context, a preparation of stabilized sulforaphane 340 μmol daily has recently been given to men with biochemical recurrence of prostate cancer after radical prostatectomy for 6 months without any adverse effects (35). Other future considerations include a closer examination of pSTAT3 molecular markers, such as downstream products of the Nrf2 transcription factor (e.g., heme oxygenase, GST) in the study of the pharmacodynamics of oral BSE-SFN. Further study to better evaluate the effects of this agent upon the morphology, histopathology, and signaling pathways of atypical nevi is now reasonable.

Disclosure of Potential Conflicts of Interest

J.H. Beumer has ownership interest (including patents) in a patent on sulforaphane. H. Tawbi is a consultant/advisory board member for BMS, Genentech, Merck, and Novartis. J.M. Kirkwood is a consultant/advisory board member for Amgen, Array Biopharma, BMS, Immunocore, Merck, Novartis, and Roche. No potential conflicts of interest were disclosed by the other authors.

Authors' Contributions

Conception and design: S.V. Singh, Y. Lin, J.H. Beumer, C. Sander, S.A. Leachman, J.M. Kirkwood

Development of methodology: J.H. Beumer, S.M. Christner, J.W. Fahey, J.M. Kirkwood

Acquisition of data (provided animals, acquired and managed patients, provided facilities, etc.): J.H. Beumer, S.M. Christner, A.A. Tarhini, H. Tawbi, L.K. Ferris, J.W. Fahey, P.B. Cassidy, L.H. Butterfield, H.M. Zarour, J.M. Kirkwood

Analysis and interpretation of data (e.g., statistical analysis, biostatistics, computational analysis): S. Tahata, S.V. Singh, Y. Lin, E.-R. Hahm, J.H. Beumer, C.M. Dietz, E. Hughes, J.W. Fahey, S.A. Leachman, L.H. Butterfield, H.M. Zarour, J.M. Kirkwood

Writing, review, and/or revision of the manuscript: S. Tahata, S.V. Singh, Y. Lin, J.H. Beumer, A.A. Tarhini, H. Tawbi, L.K. Ferris, E. Hughes, J.W. Fahey, S.A. Leachman, L.H. Butterfield, J.M. Kirkwood

Administrative, technical, or material support (i.e., reporting or organizing data, constructing databases): E.-R. Hahm, J.M. Kirkwood

Study supervision: A. Rose, U.N. Rao, S.A. Leachman, J.M. Kirkwood

Other (reviewed and analyzed all histomorphologic features of the melanocytic nevi and recorded the changes as the pathologist on this study; also captured digital images of the lesions): M. Wilson, A. Rose, U.N. Rao

Other (provided lab facilities for a portion of the experiments): S.A. Leachman

Acknowledgments

This work was supported by NIH R21CA161951- Pilot Clinical-Pathological and Molecular Analysis of Atypical Nevi in Response to BSE-L-Sulforaphane. This project used the UPMC Hillman Cancer Center Cancer Pharmacokinetics and Pharmacodynamics Facility (CPPF) and Immunologic Monitoring and Cellular Products Laboratory (IMCPL) supported in part by award P30CA047904. We would like to acknowledge Lisa Huntley and Victoria Alisasis for their assistance in the preparation of this manuscript. We would also like to thank Mike Hoffelder, Dr. Paul Haley, and Kevin Mitchell from Computer Vision Group, Veytel, LLC for their expertise in performing the nevus image analysis, and Dr. Robert Parise for his assistance with modifications to the liquid chromatographic-mass spectrometric assay.

The costs of publication of this article were defrayed in part by the payment of page charges. This article must therefore be hereby marked *advertisement* in accordance with 18 U.S.C. Section 1734 solely to indicate this fact.

Received August 22, 2017; revised December 29, 2017; accepted April 18, 2018; published first April 24, 2018.

References

1. American Cancer Society. Cancer Facts & Figures 2016. Atlanta, GA: American Cancer Society, 2016.
2. Miller AJ, Mihm MC Jr. Melanoma. N Engl J Med 2006;355:51–65.
3. Kang S, Barnhill RL, Mihm MC Jr, Fitzpatrick TB, Sober AJ. Melanoma risk in individuals with clinically atypical nevi. Arch Dermatol 1994;130:999–1001.
4. Perkins A, Duffy RL. Atypical moles: diagnosis and management. Am Fam Physician 2015;91:762–7.
5. Elder DE, Green MH, Guerry D, Kraemer KH, Clark WH Jr. The dysplastic nevus syndrome: our definition. Am J Dermatopathol 1982;4:455–60.
6. Begg CB, Orlow I, Hummer AJ, Armstrong BK, Kricker A, Marrett LD, et al. Lifetime risk of melanoma in CDKN2A mutation carriers in a population-based sample. J Natl Cancer Inst 2005;97:1507–15.
7. Bishop DT, Demenais F, Goldstein AM, Bergman W, Bishop JN, Bressac-de Paillerets B, et al. Geographical variation in the

penetrance of CDKN2A mutations for melanoma. J Natl Cancer Inst 2002;94:894–903.
8. Titus-Ernstoff L, Duray PH, Ernstoff MS, Barnhill RL, Horn PL, Kirkwood JM. Dysplastic nevi in association with multiple primary melanoma. Cancer Res 1988;48:1016–8.
9. Demierre MF, Nathanson L. Chemoprevention of melanoma: an unexplored strategy. J Clin Oncol 2003;21:158–65.
10. Francis SO, Mahlberg MJ, Johnson KR, Ming ME, Dellavalle RP. Melanoma chemoprevention. J Am Acad Dermatol 2006;55: 849–61.
11. Jensen JD, Wing GJ, Dellavalle RP. Nutrition and melanoma prevention. Clin Dermatol 2010;28:644–9.
12. Verhoeven DT, Goldbohm RA, van Poppel G, Verhagen H, van den Brandt PA. Epidemiological studies on brassica vegetables and cancer risk. Cancer Epidemiol Biomarkers Prev 1996;5:733–48.
13. Steinmetz KA, Potter JD. Vegetables, fruit, and cancer prevention: a review. J Am Diet Assoc 1996;96:1027–39.
14. van Poppel G, Verhoeven DT, Verhagen H, Goldbohm RA. Brassica vegetables and cancer prevention: epidemiology and mechanisms. Adv Exp Med Biol 1999;472:159–68.
15. Beecher CW.Cancer preventive properties of varieties of *Brassicaoleracea*: a review. Am J Clin Nutr 1994;59:1166S–70S.
16. Zhang Y, Kensler TW, Cho CG, Posner GH, Talalay P. Anticarcinogenic activities of sulforaphane and structurally related synthetic norbornyl isothiocyanates. Proc Natl Acad Sci U S A 1994;91:3147–50.
17. Fimognari C, Hrelia P. Sulforaphane as a promising molecule for fighting cancer. Mutat Res 2007;635:90–104.
18. Singh SV, Warin R, Xiao D, Powolny AA, Stan SD, Arlotti JA, et al. Sulforaphane inhibits prostate carcinogenesis and pulmonary metastasis in TRAMP mice in association with increased cytotoxicity of natural killer cells. Cancer Res 2009;69:2117–25.
19. Kirkwood JM, Farkas DL, Chakraborty A, Dyer KF, Tweardy DJ, Abernethy JL, et al. Systemic interferon-α (IFN-α) treatment leads to Stat3 inactivation in melanoma precursor lesions. Mol Med 1999;5:11–20.
20. Wheeler SE, Suzuki S, Thomas SM, Sen M, Leeman-Neill RJ, Chiosea SI, et al. Epidermal growth factor receptor variant III mediates head and neck cancer cell invasion via STAT3 activation. Oncogene 2010;29:5135–45.
21. Dhir R, Ni Z, Lou W, DeMiguel F, Grandis JR, Gao AC. Stat3 activation in prostatic carcinomas. Prostate 2002;51:241–6.
22. Abou-Ghazal M, Yang DS, Qiao W, Reina-Ortiz C, Wei J, Kong LY, et al. The incidence, correlation with tumor-infiltrating inflammation, and prognosis of phosphorylated STAT3 expression in human gliomas. Clin Cancer Res 2008;14:8228–35.
23. Moschos SJ, Edington HD, Land SR, Rao UN, Jukic D, Shipe-Spotloe J, et al. Neoadjuvant treatment of regional stage IIIB melanoma with high-dose interferon alfa-2b induces objective tumor regression in association with modulation of tumor infiltrating host cellular immune responses. J Clin Oncol 2006;24:3164–71.
24. Wang W, Edington HD, Rao UN, Jukic DM, Land SR, Ferrone S, et al. Modulation of signal transducers and activators of transcription 1 and 3 signaling in melanoma by high-dose IFNα2b. Clin Cancer Res 2007;13:1523–31.
25. Wang W, Edington HD, Rao UN, Jukic DM, Wang H, Shipe-Spotloe JM, et al. STAT3 as a biomarker of progression in atypical nevi of patients with melanoma: dose-response effects of systemic IFNalpha therapy. J Invest Dermatol 2008;128:1997–2002.
26. Talalay P, Fahey JW, Healy ZR, Wehage SL, Benedict AL, Min C, et al. Sulforaphane mobilizes cellular defenses that protect skin against damage by UV radiation. Proc Natl Acad Sci U S A 2007; 104:17500–5.
27. Dinkova-Kostova AT, Jenkins SN, Fahey JW, Ye L, Wehage SL, Liby KT, et al. Protection against UV-light-induced skin carcinogenesis in SKH-1 high-risk mice by sulforaphane-containing broccoli sprout extracts. Cancer Lett 2006;240:243–52.
28. Knatko EV, Ibbotson SH, Zhang Y, Higgins M, Fahey JW, Talalay P, et al. Nrf2 activation protects against solar-simulated ultraviolet radiation in mice and humans. Cancer Prev Res 2015;8: 475–86.
29. Fahey JW, Zhang Y, Talalay P. Broccoli sprouts: an exceptionally rich source of inducers of enzymes that protect against chemical carcinogens. Proc Natl Acad Sci U S A 1997;94:10367–72.
30. Shapiro TA, Fahey JW, Wade KL, Stephenson KK, Talalay P. Chemoprotective glucosinolates and isothiocyanates of broccoli sprouts: metabolism and excretion in humans. Cancer Epidemiol Biomarkers Prev 2001;10:501–8.
31. Shapiro TA, Fahey JW, Dinkova-Kostova AT, Holtzclaw WD, Stephenson KK, Wade KL, et al. Safety, tolerance, and metabolism of broccoli sprout glucosinolates and isothiocyanates: a clinical phase I study. Nutr Cancer 2006;55:53–62.
32. Alumkal JJ, Slottke R, Schwartzman J, Cherala G, Munar M, Graff JN, et al. A phase II study of sulforaphane-rich broccoli sprout extracts in men with recurrent prostate cancer. Invest New Drugs 2015;33:480–9.
33. Fahey JW, Wade KL, Wehage SL, Holtzclaw WD, Liu H, Talalay P, et al. Stabilized sulforaphane for clinical use: phytochemical delivery efficiency. Mol Nutr Food Res 2017;61.
34. Fahey JW, Holtzclaw WD, Wehage SL, Wade KL, Stephenson KK, Talalay P. Sulforaphane bioavailability from glucoraphanin-rich broccoli: control by active endogenous myrosinase. PLoS One 2015;10:e0140963.
35. Cipolla BG, Mandron E, Lefort JM, Coadou Y, Della Negra E, Corbel L, et al. Effect of sulforaphane in men with biochemical recurrence after radical prostatectomy. Cancer Prev Res 2015;8: 712–9.
36. Wang H, Lin W, Shen G, Khor TO, Nomeir AA, Kong AN. Development and validation of an LC-MS-MS method for the simultaneous determination of sulforaphane and its metabolites in rat plasma and its application in pharmacokinetic studies. J Chromatogr Sci 2011;49:801–6.
37. Zhang SY, Caamano J, Cooper F, Guo X, Klein-Szanto AJ. Immunohistochemistry of cyclin D1 in human breast cancer. Am J Clin Pathol 1994;102:695–8.
38. Hahm ER, Lee J, Kim SH, Sehrawat A, Arlotti JA, Shiva SS, et al. Metabolic alterations in mammary cancer prevention by withaferin A in a clinically relevant mouse model. J Natl Cancer Inst 2013;105:1111–22.
39. Brooks JD, Paton VG, Vidanes G. Potent induction of phase 2 enzymes in human prostate cells by sulforaphane. Cancer Epidemiol Biomarkers Prev 2001;10:949–54.
40. Veeranki OL, Bhattacharya A, Marshall JR, Zhang Y. Organ-specific exposure and response to sulforaphane, a key chemopreventive ingredient in broccoli: implications for cancer prevention. Br J Nutr 2013;109:25–32.
41. Nestorov IA, Aarons LJ, Arundel PA, Rowland M. Lumping of whole-body physiologically based pharmacokinetic models. J Pharmacokinet Biopharm 1998;26:21–46.
42. Shen DD. Toxicokinetics. In:Klaassen CD, editor. Casarett and Doull's toxicology: the basic science of poisons. 7th edition. New York, NY: McGraw-Hill; 2008. p. 305–26.
43. Gerami P, Yao Z, Polsky D, Jansen B, Busam K, Ho J, et al. Development and validation of a noninvasive 2-gene molecular assay for cutaneous melanoma. J Am Acad Dermatol 2017;76: 114–20.

Published OnlineFirst April 24, 2018; DOI: 10.1158/1940-6207.CAPR-17-0268

Published OnlineFirst April 24, 2018; DOI: 10.1158/1940-6207.CAPR-17-0268

Cancer Prevention Research

Evaluation of Biodistribution of Sulforaphane after Administration of Oral Broccoli Sprout Extract in Melanoma Patients with Multiple Atypical Nevi

Shawn Tahata, Shivendra V. Singh, Yan Lin, et al.

Cancer Prev Res 2018;11:429-438. Published OnlineFirst April 24, 2018.